

PACS numbers: 72.25.Dc, 71.70.Ej, 85.75.Hh

Perhaps the gate-voltage tunability of the RSO strength, quite successfully demonstrated in InGaAs/InAlAs-based (Ref. 10) and GaAs/AlAs-based (Refs. 11 and 12) quantum wells (QWs), determines the precession rate of the injected electron spin, and is therefore the most important key to the realization of the SFET. However, more than a decade of struggle has still yielded disappointing results. Its failure may be ascribed to the so far less successful factors:³ (i) efficient spin injection rate and (ii) uniformity of the RSO interaction. Apart from the most challenging issue—the spin injection problem, nonuniformity of the RSO coupling arising from the inherent random distribution of ionized dopants in the vicinity of the 2DEG plane has recently attracted certain attention to reexamine the Rashba 2DEG systems.^{8,9} This implies that the RSO coupling strength should be treated as position dependent, and the corresponding modification to, e.g., spin precession rate, in the Rashba channel must be taken into account.

when detected at \mathbf{r}_d after a straight space evolution $\mathbf{r}_1 \rightarrow \mathbf{r}_d$. Here, \mathbf{j}_{s_i} is a given spinor describing the spin injected at

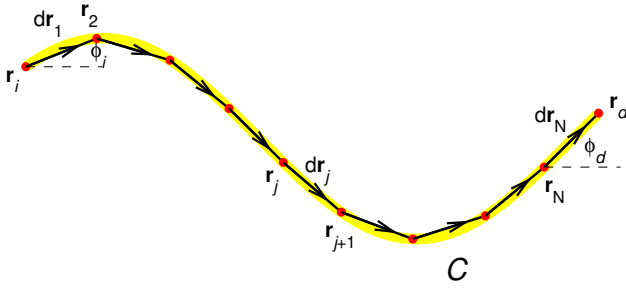


FIG. 1: (Color online) Schematic of a continuous curved path sectioned into N pieces.

\mathbf{r}_i , \mathbf{k} is the average of the two projected spin-dependent wave vector given by Eq. (A4), and

$$\mathbf{j} = \mathbf{j}(\mathbf{r}_d, \mathbf{r}_i) = \frac{1}{2} \mathbf{e}^{i\phi}(\mathbf{r}_d, \mathbf{r}_i) \quad (2)$$

is the RD eigenspinor with $\mathbf{r}_d, \mathbf{r}_i$ being the argument of the displacement vector $\mathbf{r}_d - \mathbf{r}_i$ and $\phi(\mathbf{r}_d, \mathbf{r}_i) = \arg[(\cos \phi + i \sin \phi) + i(\sin \phi + \cos \phi)]$. The phase difference is defined by

$$\phi = \frac{2}{\hbar} m^* \mathbf{r} \cdot \mathbf{r}, \quad (3)$$

where

$$\mathbf{r} = \frac{P}{\sqrt{2 + 2 + 2} \sin(2\phi)} \quad (4)$$

is the composite spin-orbit coupling strength. Note that in this paper the spatially evolved state ket without superscript, say $|\mathbf{r}_i\rangle$, means space evolution from position \mathbf{r}_i to position \mathbf{r}_2 through the straight path connecting the two points, while $|\mathbf{r}_i\rangle^C$ means evolution through path C .

For the nonuniform case, we consider an arbitrary continuous path C connecting the injection and detection points, and section the path into N pieces (see Fig. 1). In the limit of $N \rightarrow 1$, each section approaches to a straight path with constant \mathbf{r} , \mathbf{m}^* , and Eqs. (1) and (3) are then applicable

for each section. Again, we inject a spin at \mathbf{r}_i and detect the spin at \mathbf{r}_d through, however, the curved path C along which the parameters \mathbf{r} , \mathbf{m}^* may be functions of position. After successive application of Eq. (1), we obtain (see Appendix B)

$$|\mathbf{r}_i\rangle^C = \exp\left[\frac{i}{2} \int_C \mathbf{h} \cdot \mathbf{j}(\mathbf{r}_i, \mathbf{r}_d) d\mathbf{r}\right] |\mathbf{r}_d\rangle, \quad (5)$$

where the total phase difference is given by a contour integral

$$\phi = \frac{2}{\hbar} \int_C m^* \mathbf{r} \cdot d\mathbf{r}. \quad (6)$$

Compared to the uniform case Eqs. (1) and (3), the problem of nonuniform systems is simply extended to integrate the total phase difference encountered by the electron along the path C .

We remind here that the above formalism (and later the derived spin vector formula) is applicable for nonuniform systems but only with continuous spatial evolution. Propagation along discontinuous paths must be handled by sectioning the path into pieces of continuous ones [since Eq. (B6) does not hold on discontinuous points]. Another discontinuity that may crash the above formalism is the reverse of the RD field direction [at which Eq. (B6) also fails]. In pure Rashba (such as Si-Si_xGe_{1-x} asymmetric QWs) cases, the change of sign $\mathbf{r} \rightarrow -\mathbf{r}$, due to either the random dopants or the reverse gating induces such discontinuity. In the composite case (both \mathbf{r} and \mathbf{m}^* nonvanishing), the cancellation of the momentum dependence of the RD effective magnetic field at the condition $\mathbf{j} \cdot \mathbf{j} = 0$ provides possibility to run the SFET in the nonballistic regime¹³ and also contains fundamental physical phenomena.¹⁴ However, the corresponding field direction may become unstable along $[1\bar{1}0]$ or $[110]$ directions, even though the field magnitude is still continuous. When dealing with such systems, one must carefully check the continuity of the RD field direction and do the calculation partitively.

Now we apply Eq. (5) to perform the spin expectation values $\langle \mathbf{S} \rangle = \frac{\hbar}{2} \langle \mathbf{r} \rangle$, where \mathbf{r} is the Pauli matrix vector $(\mathbf{r}_x; \mathbf{r}_y; \mathbf{r}_z)$. After some mathematical manipulation, we obtain

$$\langle \mathbf{r} \rangle = \frac{1}{A} \begin{pmatrix} \cos \phi_s \cos \phi'_d \sin \phi'_i + \sin \phi_s \cos \phi'_d \cos \phi'_i + \cos \phi_s \sin \phi'_d \sin \phi'_i + \sin \phi_s \sin \phi'_d \cos \phi'_i \\ \cos \phi_s \sin \phi'_d \sin \phi'_i + \sin \phi_s \sin \phi'_d \cos \phi'_i \\ \cos \phi_s \cos \phi'_i + \sin \phi_s \cos \phi'_i \sin \phi'_d \end{pmatrix} \quad (7)$$

with $\phi'_i = \arg[(\cos \phi_i + i \sin \phi_i) + i(\sin \phi_i + \cos \phi_i)]$ and ϕ_s being the polar and azimuthal angles of the injected spin, respectively.

Clearly, Eq. (7) recovers the previous spin vector formula¹⁵ when \mathbf{r} , \mathbf{m}^* , and \mathbf{A} are constants, i.e., uniform spin precession along straight paths.

III. RESULTS AND DISCUSSION

In this section we apply our generalized version of spin-vector formula Eq. (7) with the total phase given by Eq. (6) first to some interesting 1D geometries, including quantum rings and quantum wires, and then to a more realistic 2DEG case, where position dependent RSO coupling, generated by regular and random distributions of ionized dopants, is present. In all cases, we assume constant DSO coupling and the electron effective mass.

A. 1D quantum ring

Beginning with an ideal Rashba half-ring with ring radius $0.1 \text{ } \mu\text{m}$, we inject an electron at one end, and detect $\hbar S_z$ down the way along the ring to the other end. The half-ring is assumed to be ideally 1D and made of InGaAs-based materials. We set the RSO parameter $\alpha = 0.03 \text{ eV nm}$ and the electron effective mass $m^* = 0.03 m_e$.¹⁶ Two configurations of the injected spin are considered. In ring (i) of Fig. 2(a), we inject the spin with polarization parallel to the radial direction, which is also the eigenstate of this Rashba ring case. As expected, the spin vectors maintain in the radial direction since the spin is injected in its eigenstate and will stay in this state

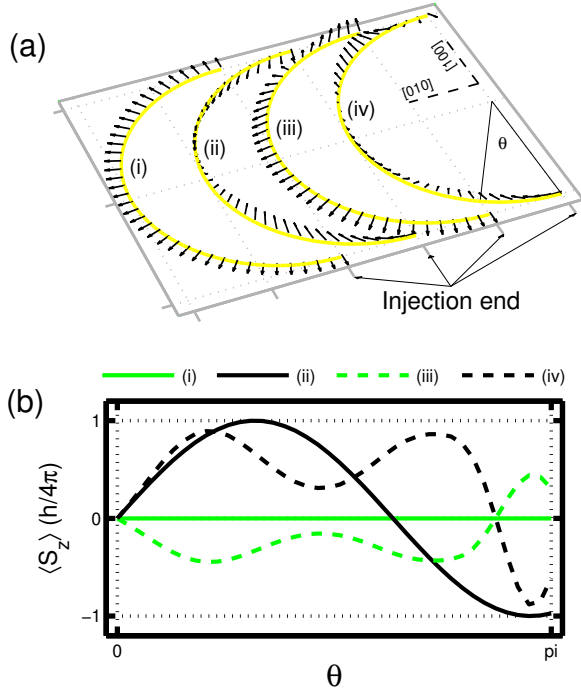


FIG. 2: (Color online) (a) Spin vectors along four ideal 1D half-rings. Rings (i) and (ii) contains only the RSO while in rings (iii) and (iv) the DSO is involved. The spin, polarized parallel either to the radial or the tangential directions, is injected at the lower end of each ring. (b) Corresponding $\hbar S_z$ in units of $\hbar/4\pi$ as a function of the ring argument θ .

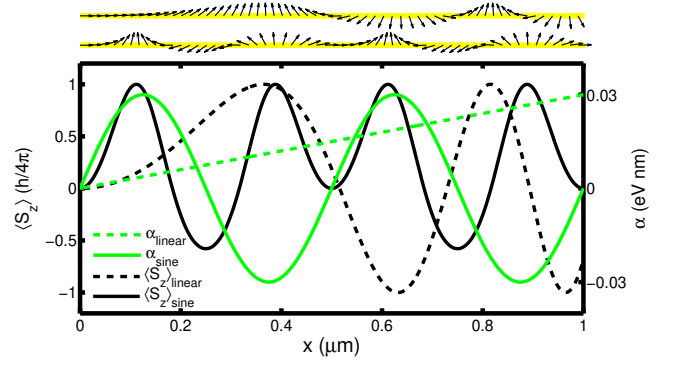


FIG. 3: (Color online) Two ideal 1D wires with position-dependent RSO strength. The upper wire shows the effect of a linear and the lower wire shows a sine-varying α . In the main panel, α and $\hbar S_z$ as functions of the longitudinal position are plotted.

hereafter. This can also be viewed as a generalized version of our previous proposal of precessionless spin transport wire.¹⁷ In Rashba systems, one can precessionlessly transport spins even through an arbitrary wire shape (but with continuous curvature), once the spin is injected with polarization perpendicular to the wire direction.

Next we inject the spin parallel to the tangential direction. As shown in ring (ii) of Fig. 2(a), the injected spin precesses upright down the way to the end. This is equivalent to the Datta-Das SFET with a curved 1D Rashba channel. Whereas the RSO coupling induces an effective magnetic field \mathbf{B}_{eff} , which is always perpendicular to the electron transport ($\mathbf{B}_{\text{eff}} \perp \mathbf{k}$ the radial direction here), rings (i) and (ii) in Fig. 2(a) are both reasonable and expectable. However, when the DSO coupling is involved, the z-rotational symmetry is broken, and the spin vectors cannot be expected intuitively, but can still be well described by our formula Eq. (7) [see rings (iii) and (iv) in Fig. 2(a)]. To clarify the influence due to the DSO, we plot $\hbar S_z$ as a function of the ring argument θ in Fig. 2(b), where line (i) and line (ii) exhibit precessionless and complete precessing behaviors, respectively, and change to line (iii) and line (iv) after getting the DSO coupling involved.

B. 1D quantum wire

We now consider two straight quantum wires with position-dependent RSO strength, one being a linear wire and the other a sine-varying wire. These wires exhibit interesting spin precession behaviors, as shown in Fig. 3, where the upper and lower wires, sketched from the side view, correspond to the linear and sine-varying Rashba wires, respectively. As expected, the injected spin rotates with a precession rate increasing with the position, in the linear Rashba wire. In the sine case, the alternate positive and negative RSO drives the spin to precess backward (when $\alpha > 0$) and forward (when $\alpha < 0$). These quantum wires may be fabricated by special gating designs, but applicability to the spintronic device is not obvious. However, the physics indicated here is sim-

ple and clear. Whereas the magnitude of the RSO strength determines the spin precession rate, the sign of α controls the precession direction. From the viewpoint of gating, a strong enough backgate may reverse the electric field direction in the 2DEG, and hence the resulting Rashba field direction, forcing the spin to precess in an opposite direction. From the viewpoint of the random Rashba field, such an alternate α is similar to that in a symmetric quantum well, e.g., a Si-Si_xGe_{1-x} well, and will induce a finite spin relaxation rate.⁸

C. 2DEG channel with regular and random dopants: Random Rashba effect

Finally, we arrive at the crucial but realistic problem: how will the spin precession pattern be modified due to the random Rashba field? A first guess on the basis of Eq. (6) is that how wide the angle the spin precesses through lies in how much spin-orbit interaction the electron encounters along the path it goes. A symmetric well, which has a vanishing spatially averaged RSO $\langle \alpha \rangle = 0$, does not have spin precession pattern within a submicrometer scale, even though there are nonvanishing fluctuating Rashba fields. This is similar to the sine-varying Rashba wire shown in Fig. 3 but with a much rapid oscillation period (\sim atomic sizes). We now consider an asymmetric well, and adopt the same principle introduced by Sherman *et al.*⁹ to generate the random Rashba field.

Specifically, we consider a 400 nm \times 267 nm InAs-based 2DEG with only a single dopant layer, located at a spacing $z_0 = 20$ nm from the conducting plane. Within the dopant layer, charged dopant atoms are randomly distributed, generating the Coulomb field with z component described by $E_z(\mathbf{r}) = e z_0 \sum_j \frac{1}{|\mathbf{r} - \mathbf{r}_j|^{3/2}}$. Here e is the electron charge, ϵ_0 is the material permittivity, $\mathbf{r} = (x, y)$ is the two-dimensional position vector, and \mathbf{r}_j is the position of the j th dopant. We take the dopant concentration $n = 2.5 \times 10^{11} \text{ cm}^{-2}$ (same with Ref. 9), the permittivity $\epsilon_0 = 15\epsilon_0$ (ϵ_0 is the free space permittivity), and the lattice constant $a = 0.6058 \text{ nm}$.¹⁸ Using the linear model $\alpha(\mathbf{r}) = s_0 E_z(\mathbf{r})$ with $s_0 = 110 \text{ \AA}^2$ for InAs,^{11,19} we obtain the Rashba field in the cases of regular and random dopant distributions in Figs. 4(a) and 4(b), respectively.

In the 2DEG channel, we also take into account the DSO coupling by assuming the well thickness $w = 50 \text{ \AA}$, leading to $k_z^2 = 1.062 \times 10^3 \text{ eV nm}^{-1}$. Here $\alpha = 26.9 \text{ eV \AA}^3$ for InAs QWs (Ref. 11) and $k_z^2 = (\frac{m^*}{m})^2$ in the case of rigid walls. Assuming point injection of x -polarized spins at the left-center of the channel with transport direction $[110]$, the spin vector formula Eq. (7) gives the spin precession patterns, as shown in Fig. 4(c) for the regular channel and Fig. 4(d) for the random channel. Clearly, the randomness of the dopant distribution distorts the precession pattern, and hence is expected to lower the purity of the spin signal collected at the drain end. This may bring another difficulty in realizing the Datta-Das transistor.¹ Moreover, such unpredictable random distribution will eventually cause an uncertainty of the collected spin signal, for each individual 2DEG channel,

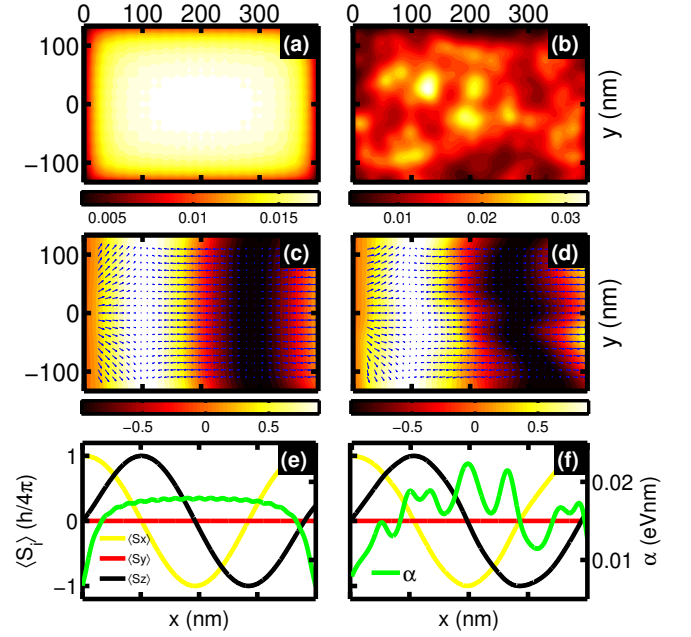


FIG. 4: (Color online) Position-dependent Rashba field with (a) regular and (b) random dopant distribution, resulting in the corresponding spin precession patterns in (c) and (d), respectively, where point injection of x -polarized spins at the left ends, are assumed. The color bars determine the magnitude of α in units of eV nm in (a) and (b), and the z component of the spin vector $\hbar S_z$ in units of $\hbar/2$ in (c) and (d). (e) and (f) show $\hbar S_x$, $\hbar S_y$, $\hbar S_z$; and α as functions of longitudinal position x at $y = 0$ for the regular and the random cases, respectively.

even if the dopant concentration is perfectly controlled. For example, the standard deviation calculation with the 2DEG channel conditions considered here shows that $S_x = (\sim 2) \times 10^{-1}$ for InAs-based and $S_x = (\sim 2) \times 10^{-2}$ for GaAs-based materials. (Here S_x means the standard deviation of the averaged x component of the spin signal collected at the drain end in the channel, among a number of different samplings.)

Note that we have chosen $[110]$ as the channel direction, where the Rashba and Dresselhaus fields are parallel,¹⁵ and the random effect seems moderate. When analyzing other channel directions such as $[1\bar{1}0]$, the obtained spin precession pattern will be totally different from the regular case. Last, if we go back to the 1D case and focus on the center path from the source end to the drain end, the distortion of the spin precession curves due to the random Rashba field is surprisingly weak [see Figs. 4(e) and 4(f)]. This again supports the suggestion of using 1D or quasi-1D channels for the Datta-Das transistor.^{1,20}

IV. SUMMARY

In conclusion, we have derived an analytical formula to describe the spin precession in nonuniform RD 2DEGs, using a

contour-integral method. The obtained results are applicable for 2DEG systems with position-dependent α , β , and m^* , and curved 1D wires. Numerical examples show interesting spin precession behaviors, and also support the idea of the precessionless spin transport wire¹⁷ in the Rashba ring case. We have also demonstrated how the spin precession pattern in a RD 2DEG may be distorted when taking the random Rashba field into account. In the viewpoint of carrying out the SFET, the random Rashba effect may distort the regular spin precession pattern in the 2DEG channel, especially along weak spin-orbit strength directions. Such undesired influence can be suppressed quite well when narrowing down the channel to 1D [compare Figs. 4(f) with 4(e)], supporting the pioneering suggestions of using quasi-1D channels.^{1,20}

Acknowledgments

One of the authors (M.H.L.) is grateful to Son-Hsien Chen and Ivo Klik for valuable discussions and suggestions. This work is supported by the Republic of China National Science Council Grant No. 94-2112-M-002-004.

APPENDIX A: UNIFORM SPACE EVOLUTION ALONG STRAIGHT PATH

To derive Eq. (1), we use the translation operator to bring the ket $|\mathbf{j}\rangle_{\mathbf{x}_i}$ from \mathbf{x}_i to \mathbf{x}_d : $|\mathbf{j}\rangle_{\mathbf{x}_d} = e^{i\mathbf{p} \cdot (\mathbf{x}_d - \mathbf{x}_i)} |\mathbf{j}\rangle_{\mathbf{x}_i}$. Expanding $|\mathbf{j}\rangle_{\mathbf{x}_i}$ in terms of the RD eigenspinors $|\mathbf{j}\rangle$; $\mathbf{x}_d - \mathbf{x}_i = \mathbf{r}$ and denoting $\mathbf{r} = \mathbf{r}_d - \mathbf{r}_i$ we have

$$|\mathbf{j}\rangle_{\mathbf{x}_d} = e^{i\mathbf{p} \cdot \mathbf{r}} (c_+ |\mathbf{j}\rangle + c_- |\mathbf{j}\rangle; \mathbf{x}_d - \mathbf{x}_i), \quad (\text{A1})$$

where $c_\pm = \langle \mathbf{j} | \mathbf{r} \rangle_{\mathbf{x}_d}$ are the expansion coefficients (\mathbf{r} is the argument angle of the vector \mathbf{r}). Note that the electron carrying momentum \mathbf{p} is supposed to move in the direction $\mathbf{x}_d - \mathbf{x}_i$, so the product $\mathbf{p} \cdot (\mathbf{x}_d - \mathbf{x}_i)$ is simplified to $\mathbf{p} \cdot \mathbf{r}_d - \mathbf{p} \cdot \mathbf{r}_i$. Defining

$$k = k_+ - k_- = \frac{2m^*}{\hbar^2}, \quad (\text{A2})$$

where k is the composite spin-orbit strength given in Eq. (4), we rewrite Eq. (A1) as

$$|\mathbf{j}\rangle_{\mathbf{x}_d} = e^{ik_+ \cdot \mathbf{r}} c_+ |\mathbf{j}\rangle + e^{ik_- \cdot \mathbf{r}} c_- |\mathbf{j}\rangle = e^{ik \cdot \mathbf{r}} \sum_{\mathbf{j}} e^{i(\mathbf{k}_+ - \mathbf{k}_-) \cdot \mathbf{r}} c_{\mathbf{j}} |\mathbf{j}\rangle; \mathbf{x}_d - \mathbf{x}_i, \quad (\text{A3})$$

with

$$k = \frac{k_+ + k_-}{2} \quad (\text{A4})$$

and $k \cdot \mathbf{r}$. Note that the common phase $e^{ik \cdot \mathbf{r}}$ will vanish when calculating expectation values. Whereas k depends on the energy the electron spin carries while k_\pm , or the phase difference $\mathbf{k}_+ - \mathbf{k}_-$, depends only on the spin-orbit strength, the physics of $|\mathbf{j}\rangle_{\mathbf{x}_d}$, such as the spatial spin precession, does not depend on the injection energy.

APPENDIX B: NONUNIFORM SPACE EVOLUTION ALONG CURVED PATH

To derive Eqs. (5) and (6), we refer to Fig. 1 where we denote $\mathbf{x}_{1(d)} = \mathbf{x}_{(N+1)}$ and successively apply Eq. (1) from the last to the first section. Taking the j th section for example, we have

$$|\mathbf{j}\rangle_{\mathbf{x}_{j+1}} = e^{ik_j \cdot \mathbf{r}} \sum_{\mathbf{j}} e^{i(\mathbf{k}_+ - \mathbf{k}_-) \cdot \mathbf{r}} |\mathbf{j}\rangle; \mathbf{x}_j, \quad (\text{B1})$$

with $\mathbf{r} = \mathbf{x}_{j+1} - \mathbf{x}_j$, $\mathbf{k}_+ = \mathbf{k}_j + \mathbf{k}_{j+1}$, and $\mathbf{k}_- = \mathbf{k}_j - \mathbf{k}_{j+1}$. Note that the RSO strength, DSO strength, and effective mass are ideally local: α_j , β_j , and m_j^* . Note also that the common phase factor outside the summation $\exp i\mathbf{k}_j \cdot \mathbf{r}$ with $\mathbf{k}_j = \mathbf{k}_j^+ + \mathbf{k}_j^- = 2\mathbf{k}_j$ may depend not only on the position \mathbf{x}_j but also on the direction \mathbf{j} due to the anisotropic Fermi contour in the general RD case. However, we will show that, as in the uniform straight case, this phase does not contribute to the spin vector $\hbar \mathbf{S}_i$. In the following we will abbreviate the RD eigenspinor $|\mathbf{j}\rangle$ to $|\mathbf{j}\rangle$ for simplicity.

For the full translation, we can start with the last section

$$|\mathbf{j}\rangle_{\mathbf{x}_1}^C = |\mathbf{j}\rangle_{\mathbf{x}_N} \sum_{\mathbf{j}} e^{i\mathbf{k}_N \cdot \mathbf{r}} e^{i(\mathbf{k}_+ - \mathbf{k}_-) \cdot \mathbf{r}} |\mathbf{j}\rangle_{\mathbf{x}_{N-1}}, \quad (\text{B2})$$

and successively substitute

$$|\mathbf{j}\rangle_{\mathbf{x}_{N-1}} = e^{ik_{N-1} \cdot \mathbf{r}} \sum_{\mathbf{j}} e^{i(\mathbf{k}_+ - \mathbf{k}_-) \cdot \mathbf{r}} |\mathbf{j}\rangle_{\mathbf{x}_{N-2}}, \quad (\text{B3a})$$

$$|\mathbf{j}\rangle_{\mathbf{x}_{N-2}} = e^{ik_{N-2} \cdot \mathbf{r}} \sum_{\mathbf{j}} e^{i(\mathbf{k}_+ - \mathbf{k}_-) \cdot \mathbf{r}} |\mathbf{j}\rangle_{\mathbf{x}_{N-3}}, \quad (\text{B3b})$$

$$|\mathbf{j}\rangle_{\mathbf{x}_1} = e^{ik_1 \cdot \mathbf{r}} \sum_{\mathbf{j}} e^{i(\mathbf{k}_+ - \mathbf{k}_-) \cdot \mathbf{r}} |\mathbf{j}\rangle_{\mathbf{x}_1}, \quad (\text{B3c})$$

into the expression Eq. (B2). Then totally we have

$$|\mathbf{j}\rangle_{\mathbf{x}_1}^C = e^{ik_N \cdot \mathbf{r}} e^{ik_{N-1} \cdot \mathbf{r}} \dots e^{ik_1 \cdot \mathbf{r}} \sum_{\mathbf{j}} e^{i(\mathbf{k}_+ - \mathbf{k}_-) \cdot \mathbf{r}} |\mathbf{j}\rangle_{\mathbf{x}_1}, \quad (\text{B4})$$

where we have further abbreviated $|\mathbf{j}\rangle$ to $|\mathbf{j}\rangle$. One must bear in mind that the shorthand $|\mathbf{j}\rangle$ actually means $|\mathbf{j}\rangle$; $|\mathbf{j}\rangle$. In Eq.

(B4), the spinor overlaps can be rearranged as $\langle \mathbf{h}_0 | \mathbf{j}_0 \rangle = \langle \mathbf{h}_0 | \mathbf{j}_0 \rangle$. For the j th bracket, the overlap reads

$$\langle \mathbf{h}_{(j)} | \mathbf{j}_{(j)} \rangle = \frac{1}{2} e^{i(\mathbf{h}_{(j)} - \mathbf{j}_{(j)}) \cdot \mathbf{r}} + \langle \mathbf{h}_{(j)} | \mathbf{j}_{(j)} \rangle. \quad (\text{B5})$$

In the limit of $N \rightarrow 1$ and the continuous condition, this overlap becomes $\langle \mathbf{h}_{(j)} | \mathbf{j}_{(j)} \rangle$ since $\mathbf{j}_{(j)} = \mathbf{j}_{(j)} \mathbf{1}$; $\mathbf{j}_{(j)} = \mathbf{j}_{(j)} \mathbf{1}$; and $\mathbf{j}_{(j)} = \mathbf{j}_{(j)} \mathbf{1}$ yield $\mathbf{j}_{(j)} = \mathbf{j}_{(j)} \mathbf{1}$, so that we have $\langle \mathbf{h}_{(j)} | \mathbf{j}_{(j)} \rangle = 1 + \langle \mathbf{h}_{(j)} | \mathbf{j}_{(j)} \rangle = 2 = \langle \mathbf{h}_{(j)} | \mathbf{j}_{(j)} \rangle$. Therefore, the spinor overlaps are reduced to

$$\langle \mathbf{h}_0 | \mathbf{j}_0 \rangle = \langle \mathbf{h}_0 | \mathbf{j}_0 \rangle = \langle \mathbf{h}_0 | \mathbf{j}_0 \rangle = \langle \mathbf{h}_0 | \mathbf{j}_0 \rangle, \quad (\text{B6})$$

leading to a greatly simplified expression

$$\langle \mathbf{j}_i^C | \mathbf{j}_d \rangle = \exp \left[i \sum_{n=1}^N \mathbf{k}_n \cdot \mathbf{r} \right] \exp \left[i \sum_{j=1}^N \frac{1}{2} \mathbf{j}_j \cdot \mathbf{h} \right] \langle \mathbf{j}_i | \mathbf{j}_d \rangle, \quad (\text{B7})$$

where we have returned the notations for the RD eigenspinors $\mathbf{j}_i = \mathbf{j}_i$ and $\mathbf{j}_d = \mathbf{j}_d$, and also the input spin $\mathbf{j}_i = \mathbf{j}_i$. Rewriting the prefactor and the total phase

into integration forms

$$\exp \left[i \sum_{n=1}^N \mathbf{k}_n \cdot \mathbf{r} \right] = \exp \left[i \int_C \mathbf{k}(\mathbf{r}) \cdot d\mathbf{r} \right], \quad (\text{B8})$$

$$\sum_{j=1}^N \frac{1}{2} \mathbf{j}_j \cdot \mathbf{h} = \frac{1}{2} \int_C \mathbf{m}(\mathbf{r}) \cdot d\mathbf{r}, \quad (\text{B9})$$

we finally obtain

$$\langle \mathbf{j}_i^C | \mathbf{j}_d \rangle = e^{i \int_C \mathbf{k}(\mathbf{r}) \cdot d\mathbf{r}} \exp \left[i \int_C \frac{1}{2} \mathbf{h} \cdot \mathbf{j}_i \right] \langle \mathbf{j}_i | \mathbf{j}_d \rangle. \quad (\text{B10})$$

Since the prefactor does not survive when doing expectation values (such as $\langle \mathbf{h} \cdot \mathbf{i} \rangle$) with the above ket, it makes no difference to express $\langle \mathbf{j}_i^C | \mathbf{j}_d \rangle$ as Eq. (5).

Although we have shown that the common phases in Eqs. (A3) and (B10) are *irrelevant* when calculating, e.g., the spin-vectors $\mathbf{h} \cdot \mathbf{i}$, we remind here that these phases will become *relevant* once superposition of different states is involved. In that case the prefactor induces oscillations due to interference between the superposed states, and is therefore not negligible, unless the inverse Fermi momentum is much larger than the system size, i.e., $k_F r \ll 1$.

- ¹ S. Datta and B. Das, Appl. Phys. Lett. **56**, 665 (1990).
- ² *Semiconductor Spintronics and Quantum Computation*, edited by D. D. Awschalom, D. Loss, and N. Samarth (Springer, Berlin, 2002).
- ³ Igor Žutić, Jaroslav Fabian, and S. Das Sarma, Rev. Mod. Phys. **76**, 323 (2004).
- ⁴ C. Kittel, *Quantum Theory of Solids* (Wiley, New York, 1963).
- ⁵ E. I. Rashba, Sov. Phys. Solid State **2**, 1109 (1960); Yu. A. Bychkov and E. I. Rashba, JETP Lett. **39**, 78 (1984).
- ⁶ G. Dresselhaus, Phys. Rev. **100**, 580 (1955).
- ⁷ V. I. Mel'nikov and E. I. Rashba, Sov. Phys. JETP **34**, 1353 (1972).
- ⁸ E. Ya. Sherman, Appl. Phys. Lett. **82**, 209 (2003); E. Ya. Sherman, Phys. Rev. B **67**, 161303(R) (2003).
- ⁹ E. Ya. Sherman and Jairo Sinova, Phys. Rev. B **72**, 075318 (2005).
- ¹⁰ J. Nitta, T. Akazaki, H. Takayanagi, and T. Enoki, Phys. Rev. Lett. **78**, 1335 (1997); T. Koga, J. Nitta, T. Akazaki, and H. Takayanagi, *ibid.* **89**, 046801 (2002).
- ¹¹ W. Knap, C. Skierbiszewski, A. Zduniak, E. Litwin-Staszewska, D. Bertho, F. Kobbi, J. L. Robert, G. E. Pikus, F. G. Pikus, S. V. Iordanskii, V. Mosser, K. Zekentes, and Yu. B. Lyanda-Geller, Phys. Rev. B **53**, 3912 (1996);
- ¹² J. B. Miller, D. M. Zumbühl, C. M. Marcus, Y. B. Lyanda-Geller,

- D. Goldhaber-Gordon, K. Campman, and A. C. Gossard, Phys. Rev. Lett. **90**, 076807 (2003); O. Z. Karimov, G. H. John, R. T. Harley, W. H. Lau, M. E. Flatté, M. Henini, and R. Airey, *ibid.* **91**, 246601 (2003).
- ¹³ J. Schliemann, J. C. Egues, and D. Loss, Phys. Rev. Lett. **90**, 146801 (2003).
- ¹⁴ Shun-Qing Shen, Phys. Rev. B **70**, 081311(R) (2004); N. A. Sinitsyn, E. M. Hankiewicz, Winfried Teizer, and Jairo Sinova, *ibid.* **70**, 081312(R) (2004).
- ¹⁵ Ming-Hao Liu, Ching-Ray Chang, and Son-Hsien Chen, Phys. Rev. B **71**, 153305 (2005); Ming-Hao Liu and Ching-Ray Chang, *ibid.* **73**, 205301 (2006).
- ¹⁶ Y. Sato, T. Kita, S. Gozu, and S. Yamada, J. Appl. Phys. **89**, 8017 (2001).
- ¹⁷ Ming-Hao Liu, Son-Hsien Chen, and Ching-Ray Chang, J. Appl. Phys. **99**, 08H707 (2006).
- ¹⁸ John H. Davies, *The Physics of Low-Dimensional Semiconductors* (Cambridge University Press, Cambridge, 1998).
- ¹⁹ E. A. de Andrada e Silva, G. C. La Rocca, and F. Bassani, Phys. Rev. B **55**, 16293 (1997).
- ²⁰ F. Mireles and G. Kirczenow, Phys. Rev. B **64**, 024426 (2001).